Biochemical and Biophysical Research Communications 460 (2015) 348–353

Contents lists available at ScienceDirect

Biochemical and Biophysical Research Communications

journal homepage: www.elsevier.com/locate/ybbrc

Transcription outcome of promoters enriched in histone variant H3.3 defined by positioning of H3.3 and local chromatin marks

Eivind G. Lund, Philippe Collas, Erwan Delbarre*

Department of Molecular Medicine, Institute of Basic Medical Sciences, Faculty of Medicine, University of Oslo, 0317 Oslo, Norway

ARTICLE INFO

Article history:
Received 21 February 2015
Available online 14 March 2015

Keywords:
Histone modification
H3.3
Gene expression
Promoter
Adipose stem cell

ABSTRACT

Replication-independent histone variant H3.3 is incorporated into distinct genomic regions including promoters. However topology of promoter-associated H3.3 in relation to chromatin modifications and transcriptional outcome is not known, providing no insight on any distinction between H3.3-containing active and inactive promoters. Here, we report algorithms providing information on gene expression status as a function of density and position of multiple chromatin marks on promoters. We identify a relationship between promoter enrichment in epitope-tagged H3.3 or its canonical isoform H3.2 and corresponding transcriptional outcomes, as a function of sub-promoter positioning of DNA methylation and H3K4me3, H3K9me3 and H3K27me3. We identify a low-frequency configuration of H3.3 and H3K9me3 co-occupancy associated with transcriptional activity, while H3.3 and H3K27me3 promoters are invariably inactive. We unveil H3.3 and DNA methylated promoters whose transcription outcome depends on H3.3 sub-promoter positioning. Our results indicate how spatially restricted positioning of H3.3 may add another layer of transcription regulation.

1. Introduction

Nucleosome composition is important for many nuclear functions including regulation of gene expression. Nucleosome properties can be modulated by post-translational modifications of histones in a manner that affects local chromatin density and binding of transcriptional regulators [1], and by inclusion of histone variants [2,3]. Eight variants of histone H3 have to date been identified, including the canonical H3.1 and H3.2 isoforms, and the H3.3 variant [4,5]. In contrast to H3.1 or H3.2 which are expressed only during S phase, H3.3 is expressed throughout the cell cycle, enabling deposition into chromatin in a replication-independent manner [6]. Delivery of H3.3 to chromatin involves distinct chaperones thought to be responsible for site-specificity of H3.3 deposition, including HIRA, ASF1 and the DAXX/ATRX complex [3].

H3.3 is notably incorporated into gene regulatory regions, through mechanisms that remain largely unknown. We have recently identified a novel pathway of deposition of epitope-tagged H3.3 into chromatin in human adipose tissue stem cells (ASCs) [7] and mapped its localization in promoters of active and inactive genes [8]. H3.3 topology on promoters relative to histone and DNA modifications and resulting transcriptional outcome has however not been examined, providing no insight on any distinction between H3.3-containing active and inactive promoters. Here, we defined algorithms providing information on the transcription outcome of genes as a function of promoter density and relative positioning of multiple chromatin modifications. We now show that spatially restricted positioning of not only chromatin marks, but also H3.3, on sub-promoter regions adds another layer of transcription regulation.

2. Materials and methods

2.1. Chromatin immunoprecipitation (ChIP), methylated DNA immunoprecipitation (MeDIP) and gene expression data

ChIP–chip data for epitope-tagged H3.3e and H3.2e [8], and MeDIP-chip and ChIP–chip data for H3K4me3, H3K9me3 and H3K27me3 [9] were previously published by us for ASCs. Gene expression was determined in a parallel study [10] for the same pool of ASCs as those used for ChIP and MeDIP. Illumina Human HT-12 v4 expression BeadChip arrays and Illumina's GenomeStudio were used to compute a detection P-value for each probe. Genes

Abbreviations: ChIP, chromatin immunoprecipitation; MeDIP, methylated DNA immunoprecipitation; H3.3e, H3.3-EGFP; H3.2e, H3.2-EGFP; TSS, transcription start site; ASCs, adipose tissue stem cells.

* Corresponding author. University of Oslo, Institute of Basic Medical Sciences, PO Box 1112 Blindern, 0317 Oslo, Norway. Fax: +47 22851058.
E-mail address: erwan.delbarre@medisin.uio.no (E. Delbarre).

http://dx.doi.org/10.1016/j.bbrc.2015.03.037
0006-291X/

with a $P < 0.01$ were considered as expressed. Signal intensities between replicates were normalized using the lumi package [11] and replicate signals combined by using median signal intensity.

2.2. Identification of H3.3e and H3.2e enrichment domains

Chromosomes were visualized as a sequence of genes ordered by TSS positioning. A 20-gene sliding window ('size 20') with step size 1 was used to determine the number of genes enriched in H3.3e or H3.2e in the window. Data for genes with multiple TSSs were collapsed into a single gene.

2.3. Density heat maps

The number of transcripts with H3.3e, H3.2e and modified histone peak at a given position relative to the TSS determined whether and where a mark had a non-uniform distribution of peaks in promoter regions. This was computed as follows:

$$f(x) = \sum_{i=1}^{n} T_{i,x}$$

where $T_{i,x}$ equals 1 if transcript i has a peak of a given type at position x relative to TSS, and equals 0 otherwise.

We expressed the relationship between relative peak position and transcription as the ratio of expressed transcripts as a function of peak position relative to the TSS, using the equation:

$$f(x) = \frac{\sum_{i=1}^{n} T_{i,x} * E_i}{\sum_{i=1}^{n} T_{i,x}}$$

where E_i equals 1 if transcript i is transcribed and equals 0 otherwise.

We also examined promoters enriched in two marks to assess whether the two marks alter the typical distribution of peaks for at least one of the marks. Determination of how peaks of two marks are positioned on the same promoter was done by extending the analysis to two dimensions:

$$f(x,y) = \sum_{i=1}^{n} T_{i,x,y}$$

where x is the position of X peaks relative to TSS, y is the position of Y peaks relative to TSS, and $T_{i,x,y}$ equals 1 if transcript i has a peak of type X at position x and a peak of type Y at position y relative to TSS.

Transcription ratio as a function of peak position relative to TSS similarly can be extended to two dimensions using the equation:

$$f(x,y) = \frac{\sum_{i=1}^{n} T_{i,x,y} * E_i}{\sum_{i=1}^{n} T_{i,x,y}}$$

where $T_{i,x,y}$ and E_i are as above.

2.4. Data access

H3.3e and H3.2e ChIP–chip and MeDIP-chip data are available under GEO GSE19773. H3 methylation ChIP–chip and gene expression data are available under GEO GSE42560.

3. Results and discussion

3.1. Epitope-tagged H3.3 targets promoters of developmentally-regulated genes, and of genes with a wide range of expression levels

To gain insight on the implication of H3.3 loading on regulatory regions and associated transcriptional output, we analyzed in a chromatin context the global and local distribution of H3.3-EGFP (designated H3.3e) and H3.2-EGFP (H3.2e) in promoters of human cultured ASCs. We used H3.3e and H3.2e promoter occupancy maps established by ChIP–chip [8], MeDIP-chip DNA methylation profiles [9], H3K4me3, H3K9me3 and H3K27me3 ChIP–chip promoter maps [9] and gene expression assessed using microarrays [9]. Promoter analysis was confined to a −2.2 to +0.5 Kb region around the TSS of 18,028 HG18 RefSeq genes, using MA2C with $P < 10^{-2}$ for peak calling for all marks. We identified 1769 and 1509 genes with a promoter enriched in H3.3e or H3.2e respectively (referred to as "H3.3e genes" and "H3.2e genes"), among which 454 overlap (Fig. 1A; Supplementary Table 1). We find that H3.2e genes are expressed at lower levels than H3.3e genes ($P = 2.5 \times 10^{-11}$; Wilcoxon rank-sum test) or RefSeq genes ($P = 3.6 \times 10^{-13}$; Fig. 1B). H3.3e genes display a range of expression levels similar to RefSeq genes ($P = 0.283$; Fig. 1B) and thus is targeted to both expressed and non-expressed genes.

H3.3e deposition on inactive promoters suggests a transcription-independent loading of H3.3. Gene Ontology analysis shows that H3.3 is notably enriched on promoters of genes with central developmental functions (P values $< 10^{-7}$; Supplementary Table 2). In a context of undifferentiated cells with multi-lineage differentiation potential, as we have shown for ASCs [12], this feature of H3.3 enrichment suggests a role in priming chromatin for transcriptional activation of signaling pathways upon ASC differentiation [13]. This may also reflect a mark of previous transcriptional activity, as some of these promoters are expressed (at low levels) in freshly isolated ASCs and down-regulated in culture [12]. Thus, H3.3e detection at inactive promoters may reflect a memory of a previous transcriptionally active state [14]. H3.3 loading on inactive sites is also consistent with a nucleosome gap filling role of HIRA, which we expect to load H3.3 in chromatin regions independently of any transcription activity [15,16].

3.2. Genes with promoters enriched in H3.3e or H3.2e are linearly clustered

We next determined whether genes enriched in H3.3e or H3.2e are clustered or uniformly distributed in the genome. We computed the number of H3.3e or H3.2e genes in a fixed 20-gene sliding window across all chromosomes. As we only have enrichment information for promoters, a window of consecutive genes (which is irrespective of distance between adjacent genes) alleviates enrichment bias due to high gene density. We find that the distribution of H3.3e and H3.2e clusters is overall distinct, with clusters enriched in H3.3e deprived of H3.2e and vice versa (Fig. 1C,D), though some overlap of H3.3e- and H3.2e-rich domains occurs (Supplementary Fig. 1A). These data indicate the existence of spatially overlapping and spatially distinct H3.3- and H3.2-enriched domains detected by ChIP, in line with previous microscopy observations [8]. Clustering of H3.3 target genes may provide a mechanism for efficient H3.3 deposition. This is consistent with spatially restricted sub-nuclear sites of enrichment for H3.3 chaperones [7]. The formation of nodes of H3.3 loading may be promoted by three-dimensional chromatin folding [17], perhaps generating regulatory networks.

3.3. Topological mapping of promoter-associated H3.3e

We find that genes with H3.3e-enriched promoters display a wide range of expression levels (Fig. 1B), indicating that H3.3 enrichment per se is not sufficient to discriminate active and inactive promoters. Factors putatively affecting expression of H3.3e promoters would include spatial positioning of H3.3 on these promoters, enrichment in specific chromatin marks and position of these marks relative the TSS.

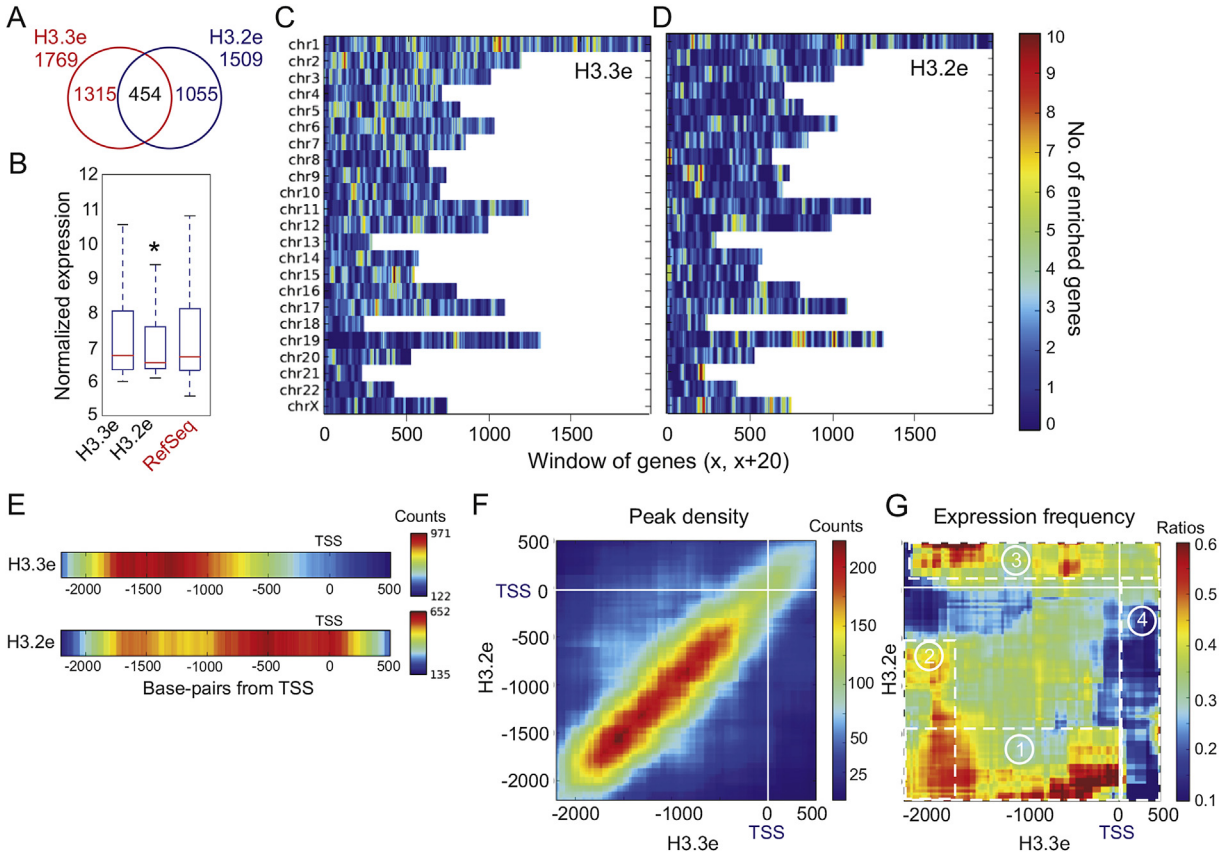

Fig. 1. Genes with H3.3e- and H3.2e-enriched promoters show clustering across the genome. (A) Venn diagram analysis of genes with a promoter enriched in H3.3e and H3.2e. (B) Median expression levels of H3.3e- and H3.2e-enriched genes. *$P = 3.6 \times 10^{-13}$ relative to RefSeq; $P = 2.5 \times 10^{-11}$ relative to H3.3e. (C, D) Distribution of H3.3e-enriched and H3.2e-enriched genes in a 20-gene sliding window (x, x + 20) across the genome. Scale shows numbers of enriched genes in the window at a given genomic position. (E) Density heat maps of H3.3e and H3.2e peaks on −2.2 Kb to +0.5 Kb of promoter region relative to the TSS. (F) 2-D density heat map of H3.3e and H3.2e peak position on co-enriched promoters (n = 454). Scale shows numbers of genes with a peak of H3.3e and H3.2e. (G) 2-D expression frequency heat map corresponding to the peak density map in (F). Scale bar shows ratios of expressed genes to all genes with a peak of H3.3e and H3.2e. Frames 1–4 represent regions shown in Fig. 4; x and y axis: distance from TSS (base pairs).

We first mapped the densities of H3.3e and H3.2e peaks across promoters by defining the midpoint of each H3.3e or H3.2e peak and computing the numbers of genes with given peak midpoint position relative to the TSS. Resulting one-dimensional (1-D) density heat maps reveal distinct profiles for H3.3e and H3.2e (Fig. 1E). H3.3e is more frequently enriched −2 to −0.5 Kb upstream of the TSS, and more seldom at the TSS or in the first 0.5 Kb downstream. In contrast, H3.2e displays broader occupancy on promoter regions including the TSS, consistent with what would be expected for a canonical core histone. Thus, H3.3e shows a preference for promoter sub-regions that exclude the TSS, whereas H3.2e displays less selectivity within promoter regions.

Second, we determined the position of the two H3 isoforms relative to each other on co-enriched promoters (n = 454; Supplementary Fig. 1B) by establishing 2-D heat maps of H3.3e and H3.2e peak densities for any given offset from the TSS. We find that both H3 variants show a strong tendency to co-localize up to −0.5 Kb from the TSS (Fig. 1F). Much less frequently are H3.3e and H3.2e spatially separated, i.e. with H3.3e distal and H3.2e proximal to or at the TSS, or vice versa (Fig. 1F, blue areas (in the web version)).

Third, to determine whether a given H3.3e and H3.2e peak position corresponds to a specific expression pattern of the corresponding gene, we constructed a 2-D gene expression heat map by calculating the ratios of expressed genes over the total number of genes with H3.3e and H3.2e peaks at a given offset from the TSS. On these maps, a given genomic coordinate projects to the same coordinate on the peak density map (Supplementary Fig. 1C). The data reveal several gene expression patterns related to the distribution of the two H3 isoforms (Fig. 1G). We observe highest expression frequency of genes with H3.3e throughout the promoter up to the TSS and H3.2e in an 'upstream-distal' location (Fig. 1G, frame 1); this configuration however affects a minor proportion of genes (Fig. 1F). We also detect high expression frequency with the opposite configuration, i.e. H3.2e on the promoter and H3.3e upstream-distal from the TSS (Fig. 1G, frame 2), again on a small number of genes. We also note expression of genes with H3.2e downstream of the TSS and H3.3e along the promoter (Fig. 1G, frame 3). Lastly, genes with H3.3e downstream of the TSS are not expressed regardless of H3.2 distribution (Fig. 1G, frame 4). These results highlight important features of H3.3e and H3.2 positioning on promoters and gene expression outcomes. H3.3 display a stricter spatial selectivity than H3.2; when co-enriched, H3.3e and H3.2e predominantly coincide, and strongest transcription output occurs when both isoforms concur upstream-distal of the TSS (−2 to −1.5 Kb; most frequent) or are spatially disjoint (a rarer occurrence).

3.4. H3.3e positioning in relation to histone and DNA methylation marks

To further investigate factors influencing the expression outcome of H3.3e-enriched promoters, we examined expression levels of genes with a promoter co-enriched in H3.3e (or H3.2e) and H3K4me3, H3K27me3, H3K9me3 or DNA methylation

(Supplementary Fig. 2). Firstly, we find a lower proportion of H3.3e than H3.2e promoters enriched in H3K9me3, H3K27me3 and DNA methylation (Fig. 2A $P < 10^{-5}$, Fisher's exact test), in line with the reported propensity of H3.2 for repressive chromatin modifications [18]. Secondly, H3.3e genes marked by H3K4me3 or DNA methylation are expressed at levels above or comparable to RefSeq genes ($P = 2.9 \times 10^{-9}$ and $P = 0.036$ respectively; Wilcoxon rank-sum test), while those marked by H3K27me3 are not expressed relative to ResSeq genes ($P = 2.2 \times 10^{-6}$; Fig. 2B). This is also the case for H3.2e genes (Fig. 2C; $P = 6.8 \times 10^{-9}$, $P = 0.567$ and $P = 6.9 \times 10^{-16}$ for H3K4me3, DNA methylation and H3K27me3 respectively). Surprisingly however, we find that H3.3e genes, but not H3.2e genes, co-enriched in H3K9me3 display a wide range of expression levels (Fig. 2B,C), suggesting that H3.3e enrichment may confer expression to a subset of H3K9me3-marked genes.

To examine this further, we established 2-D peak density heat maps of H3K4me3, H3K9me3, H3K27me3 and DNA methylation relative to H3.3e (or H3.2e), and corresponding expression frequency heat maps (Fig. 3; Supplementary Fig. 3). The data show that H3.3e most frequently coincides with the H3 methylation or DNA methylation marks examined along the promoter (Fig. 3A), suggesting that it carries the modifications. Similar observations were made for H3.2e (Supplementary Fig. 4).

As anticipated, H3.3e- and H3K4me3-marked genes are frequently expressed, particularly when H3K4me3 is enriched over the TSS (Fig. 3, frame 1). High expression frequency is also noted for H3K4me3 genes with H3.3e at the TSS and downstream (Fig. 3, frame 2). Thus, H3.3e occupancy over the TSS is compatible with expression of a subset of H3K4me3-marked genes. In contrast, H3K27me3-marked genes are essentially not expressed regardless of H3.3e distribution, consistent with H3K27me3 repressing activity of promoters. Interestingly, expression status of H3.3e and H3K9me3 co-enriched genes depends on the relative position of both marks.

H3K9me3-marked genes are overall not expressed or expressed at low levels. However, a subset of these genes is expressed, in a configuration with H3.3e upstream of the TSS (>−1.5 Kb) and H3K9me3 upstream proximal (0 to −0.5 Kb) or more distal (>−1.5 Kb; Fig. 3, frames 3, 4); H3.3e downstream is associated with a repression state (Fig. 3, frame 5). This suggests that H3K9me3-marked genes can be expressed under a specific configuration of H3K9me3 and H3.3e distribution. We make similar observations for promoters co-enriched in H3.3e and DNA methylation (Fig. 3, frames 6, 7), in line with earlier results [8,9]. Lastly, we note that expression patterns of H3.2e-enriched genes are overall similar to those of H3.3e genes albeit at slightly reduced levels (Supplementary Fig. 4).

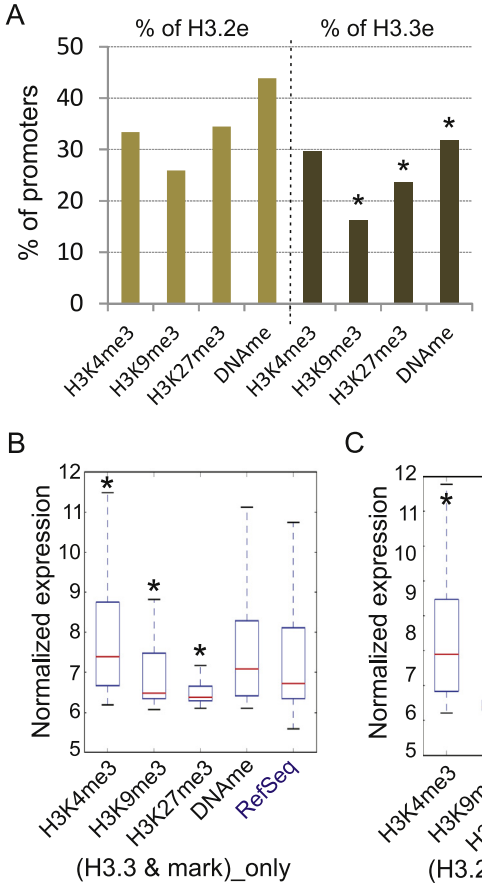

Fig. 2. Differential enrichment of H3.3e and H3.2e promoters in chromatin marks. (A) Proportions of H3.2e and H3.3e promoters enriched in H3K4me3, H3K9me3, H3K27me3 or DNA methylation. *$P < 10^{-5}$ relative to the same hPTM as percent of H3.2e; Chi-square test with Yates' correction. (B, C) Box plot analysis of expression levels of genes marked by (B) H3.3e or (C) H3.2e, and indicated chromatin modifications; *$P < 10^{-4}$ relative to RefSeq genes; Wilcoxon rank-sum test.

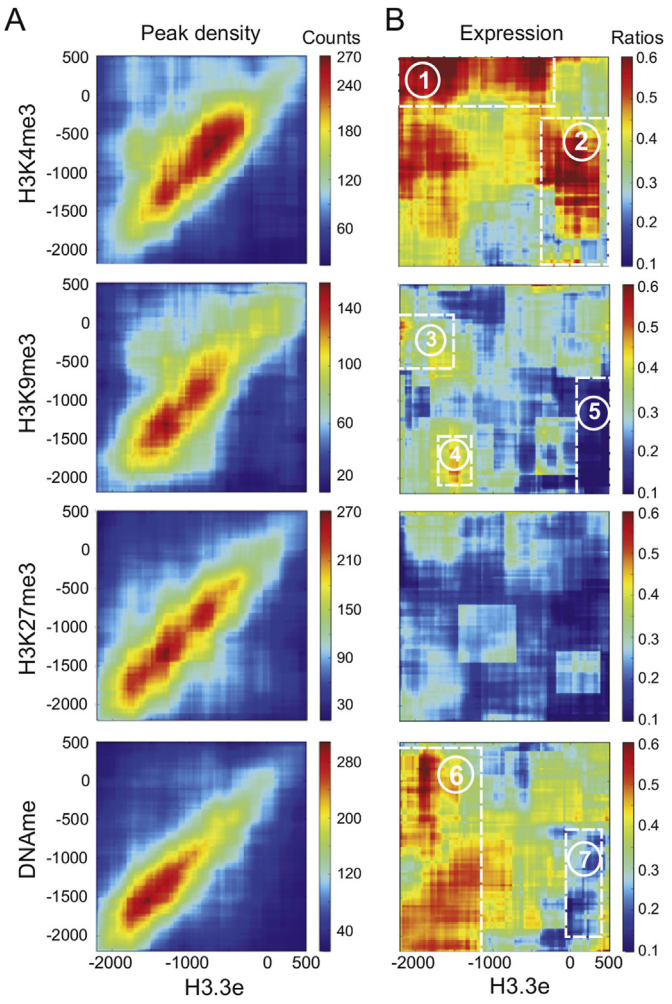

Fig. 3. H3.3e-enriched genes show distinct transcription outcomes related to positioning of H3.3e and associated chromatin modification. *Left panels*, 2-D density heat maps of peaks of H3.3e (x axis) and indicated histone or DNA methylation mark (y axis), for a given position relative to the TSS (0). *Right panels*, corresponding 2-D expression frequency heat maps. Scale bars are as in Fig. 1; x and y axis: distance from TSS (base pairs).

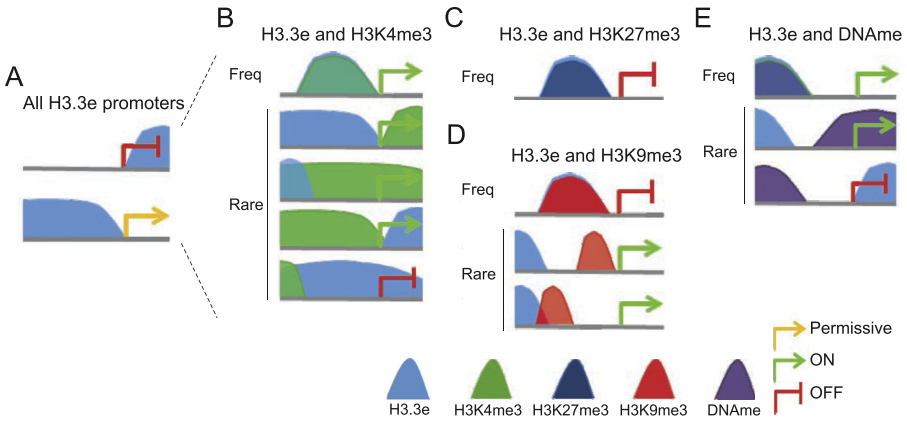

Fig. 4. Transcriptional outcomes of H3.3e-marked promoters relates to H3.3e positioning in a chromatin context. (A) Transcription outcome of all H3.3e promoters a function of H3.3 positioning relative to the TSS. (B–E) Transcription outcome of H3.3e promoters marked by (B) H3K4me3, (C) H3K27me3, (D) H3K9me3 and (E) DNA methylation.

3.5. H3.3 positioning on promoters and associated gene expression: a model

Collectively, our data indicate that H3.3e is incorporated into promoters of active and inactive genes. We propose a model where expression status correlates with positioning of H3.3e peaks relative to the TSS, in a context of distinct chromatin modifications (Fig. 4). As a rule, we find that whereas H3.3 localization on the promoter itself (that is, anywhere upstream of the TSS in the regions examined) is compatible with gene expression, whereas H3.3 enrichment at the TSS or immediately downstream is linked to promoter inactivity (Fig. 4A). Exception occurs for H3H4me3-marked promoters, for which no specific position of H3.3e is linked to a given expression outcome: most of these genes are expressed regardless of H3.3 position (Fig. 4B). Inasmuch as H3K4me3 correlates with gene activity, H3K9me3 and H3K27me3 appear to override any effect H3.3e occupancy might have on expression because these promoters are overall inactive (Fig. 4C,D). Nonetheless, a number of H3K9me3-marked promoters are associated with expressed genes (Fig. 4D); there H3.3e occupies a distal region while H3K9me3 can be anywhere on the promoter. This suggests a combinatorial influence of H3.3 marking and a histone mark on a gene expression outcome.

3.6. Which histone chaperone may mediate H3.3 loading on promoters?

Our and earlier work raises the issue of which histone chaperone might be responsible for deposition of H3.3 at promoters. Evidence points to HIRA as one candidate. Accordingly, HIRA and ASF1A mediate H3.3 loading on the *Myod1* promoter in myocytes, which may enable a permissive chromatin state for RNA polymerase II [19]. Further, deletion of HIRA in mouse embryonic stem cells negatively affects H3.3 deposition at promoters and gene bodies [20]. Additionally, HIRA co-purifies with H3.3 in a complex containing CABIN1 and UBN1 [21,22], thus these factors may also be implicated in promoter loading of H3.3. The DAXX/ATRX complex may also be a candidate, as it is associated with specific regulatory regions in an activation-dependent manner in neurons [23]. These observations suggest that chaperones loading H3.3 on regulatory elements may not only be cell type-specific, but may also depend on the nature of the promoter (e.g. constitutive vs. developmentally controlled).

Data linking

H3.2e, H3.3e, histone H3 methylation ChIP-chip data, and gene expression data were downloaded from NCBI GSE17053. MeDIP data were downloaded from NCBI GSE19795.

Conflict of interest

The authors declare no conflict of interest.

Acknowledgments

This work was supported by the Research Council of Norway, the University of Oslo, the Norwegian Center for Stem Cell research and the Norwegian Cancer Society (ED).

Transparency document

Transparency document related to this article can be found online at http://dx.doi.org/10.1016/j.bbrc.2015.03.037.

Appendix A. Supplementary data

Supplementary data related to this article can be found at http://dx.doi.org/10.1016/j.bbrc.2015.03.037.

References

[1] A.J. Ruthenburg, H. Li, D.J. Patel, C. David Allis, Multivalent engagement of chromatin modifications by linked binding modules, Nat. Rev. Mol. Cell Biol. 8 (2007) 983–994.
[2] S.J. Elsaesser, A.D. Goldberg, C.D. Allis, New functions for an old variant: no substitute for histone H3.3, Curr. Opin. Genet. Dev. 20 (2010) 110–117.
[3] E. Szenker, D. Ray-Gallet, G. Almouzni, The double face of the histone variant H3.3, Cell Res. 21 (2011) 421–434.
[4] I. Maze, K.-M. Noh, A.A. Soshnev, C.D. Allis, Every amino acid matters: essential contributions of histone variants to mammalian development and disease, Nat. Rev. Genet. 15 (2014) 259–271.
[5] T. Tamura, M. Smith, T. Kanno, H. Dasenbrock, A. Nishiyama, K. Ozato, Inducible deposition of the histone variant H3.3 in interferon-stimulated genes, J. Biol. Chem. 284 (2009) 12217–12225.
[6] K. Ahmad, S. Henikoff, The histone variant H3.3 marks active chromatin by replication-independent nucleosome assembly, Mol. Cell 9 (2002) 1191–1200.
[7] E. Delbarre, K. Ivanauskiene, T. Küntziger, P. Collas, DAXX-dependent supply of soluble (H3.3–H4) dimers to PML bodies pending deposition into chromatin, Genome Res. 23 (2013) 440–451.
[8] E. Delbarre, B.M. Jacobsen, A.H. Reiner, A.L. Sørensen, T. Küntziger, P. Collas, Chromatin environment of histone variant H3.3 revealed by quantitative imaging and genome-scale chromatin and DNA immunoprecipitation, Mol. Biol. Cell 21 (2010) 1872–1884.
[9] A.L. Sørensen, B.M. Jacobsen, A.H. Reiner, I.S. Andersen, P. Collas, Promoter DNA methylation patterns of differentiated cells are largely programmed at the progenitor stage, Mol. Biol. Cell 21 (2010) 2066–2077.
[10] E. Lund, A.R. Oldenburg, E. Delbarre, C.T. Freberg, I. Duband-Goulet, R. Eskeland, B. Buendia, P. Collas, Lamin A/C-promoter interactions specify chromatin state-dependent transcription outcomes, Genome Res. 23 (2013) 1580–1589.
[11] P. Du, W.A. Kibbe, S.M. Lin, lumi: a pipeline for processing illumina microarray, Bioinformatics 24 (2008) 1547–1548.

[12] A.C. Boquest, A. Shahdadfar, K. Frønsdal, O. Sigurjonsson, S.H. Tunheim, P. Collas, J.E. Brinchmann, Isolation and transcription profiling of purified uncultured human stromal stem cells: alteration of gene expression after in vitro cell culture, Mol. Biol. Cell 16 (2005) 1131–1141.
[13] A. Shah, A. Oldenburg, P. Collas, A hyper-dynamic nature of bivalent promoter states underlies coordinated developmental gene expression modules, BMC Genomics 15 (2014) 1186.
[14] R.K. Ng, J.B. Gurdon, Epigenetic memory of an active gene state depends on histone H3.3 incorporation into chromatin in the absence of transcription, Nat. Cell Biol. 10 (2008) 102–109.
[15] D. Ray-Gallet, A. Woolfe, I. Vassias, C. Pellentz, N. Lacoste, A. Puri, David C. Schultz, Nikolay A. Pchelintsev, Peter D. Adams, Lars E.T. Jansen, G. Almouzni, Dynamics of histone H3 deposition in vivo reveal a nucleosome gap-filling mechanism for H3.3 to maintain chromatin integrity, Mol. Cell 44 (2011) 928–941.
[16] J.I. Schneiderman, G.A. Orsi, K.T. Hughes, B. Loppin, K. Ahmad, Nucleosome-depleted chromatin gaps recruit assembly factors for the H3.3 histone variant, Proc. Natl. Acad. Sci. 109 (2012) 19721–19726.
[17] E. Lieberman-Aiden, N.L. van Berkum, L. Williams, M. Imakaev, T. Ragoczy, A. Telling, I. Amit, B.R. Lajoie, P.J. Sabo, M.O. Dorschner, R. Sandstrom, B. Bernstein, M.A. Bender, M. Groudine, A. Gnirke, J. Stamatoyannopoulos, L.A. Mirny, E.S. Lander, J. Dekker, Comprehensive mapping of long-range interactions reveals folding principles of the human genome, Science 326 (2009) 289–293.
[18] S.B. Hake, B.A. Garcia, E.M. Duncan, M. Kauer, G. Dellaire, J. Shabanowitz, D.P. Bazett-Jones, C.D. Allis, D.F. Hunt, Expression patterns and post-translational modifications associated with mammalian histone H3 variants, J. Biol. Chem. 281 (2006) 559–568.
[19] J.-H. Yang, Y. Song, J.-H. Seol, J.Y. Park, Y.-J. Yang, J.-W. Han, H.-D. Youn, E.-J. Cho, Myogenic transcriptional activation of MyoD mediated by replication-independent histone deposition, Proc. Natl. Acad. Sci. U. S. A. 108 (2011) 85–90.
[20] A.D. Goldberg, L.A. Banaszynski, K.M. Noh, P.W. Lewis, S.J. Elsaesser, S. Stadler, S. Dewell, M. Law, X. Guo, X. Li, D. Wen, A. Chapgier, R.C. DeKelver, J.C. Miller, Y.L. Lee, E.A. Boydston, M.C. Holmes, P.D. Gregory, J.M. Greally, S. Rafii, C. Yang, P.J. Scambler, D. Garrick, R.J. Gibbons, D.R. Higgs, I.M. Cristea, F.D. Urnov, D. Zheng, C.D. Allis, Distinct factors control histone variant H3.3 localization at specific genomic regions, Cell 140 (2010) 678–691.
[21] H. Tagami, D. Ray-Gallet, G. Almouzni, Y. Nakatani, Histone H3.1 and H3.3 complexes mediate nucleosome assembly pathways dependent or independent of DNA synthesis, Cell 116 (2004) 51–61.
[22] S.J. Elsaesser, C.D. Allis, HIRA and Daxx constitute two independent histone H3.3-containing predeposition complexes, Cold Spring Harb. Symp. Quant. Biol. 75 (2010) 27–34.
[23] D. Michod, S. Bartesaghi, A. Khelifi, C. Bellodi, L. Berliocchi, P. Nicotera, P. Salomoni, Calcium-dependent dephosphorylation of the histone chaperone DAXX regulates H3.3 loading and transcription upon neuronal activation, Neuron 74 (2012) 122–135.